Electronic Supplementary Information (ESI)

Maria-Gabriela Alexandru,[a] Diana Visinescu,[b] Sergiu Shova,[c] Nicolas Moliner,[d] Mario Pacheco,[d,e] Miguel Julve[d] and Francesc Lloret[d]

[a]*Department of Inorganic Chemistry, Physical Chemistry and Electrochemistry, Faculty of Applied Chemistry and Materials Science, University Politehnica of Bucharest, 1-7 Gh. Polizu Street, 011061 Bucharest, Romania*

[b]*Coordination and Supramolecular Chemistry Laboratory, "Ilie Murgulescu" Institute of Physical Chemistry, Romanian Academy, Splaiul Independentei 202, Bucharest 060021, Romania. E-mail: dianavisinescu@icf.ro*

[c]*Petru Poni" Institute of Macromolecular Chemistry, Romanian Academy, Aleea Grigore Ghica Vodă 41-A, RO-700487 Iasi, Romania*

[d]*Departament de Química Inorgànica/Instituto de Ciencia Molecular, Universitat de València, C/Catedrático José Beltrán 2, 46980 Paterna, València, Spain. E-mail: francisco.lloret@uv.es*

[e]*Facultad de Química, Universidad de la República, Av. Gral. Flores 2124, 11800 Montevideo, Uruguay.*

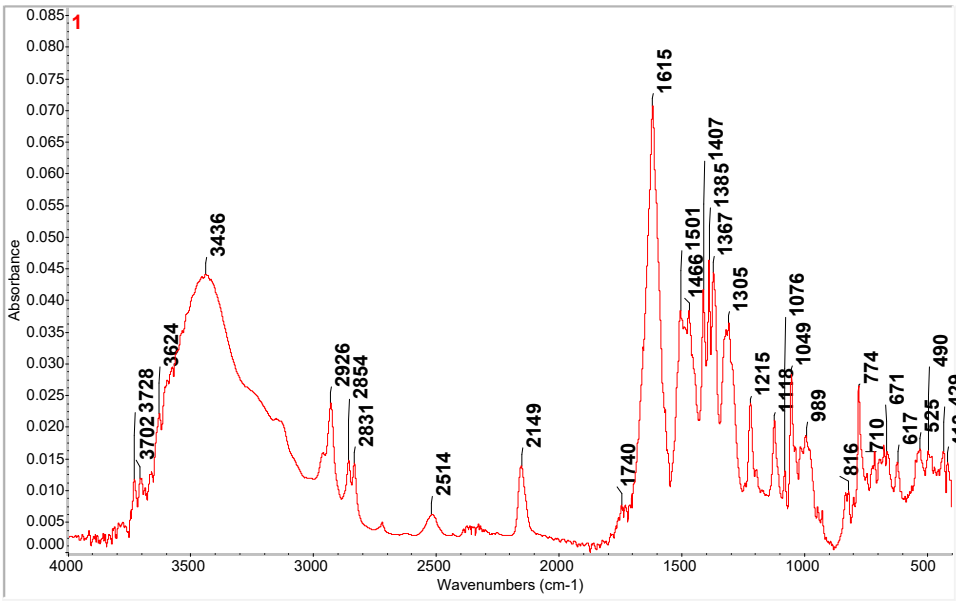

Fig. S1. FTIR spectrum of **1**.

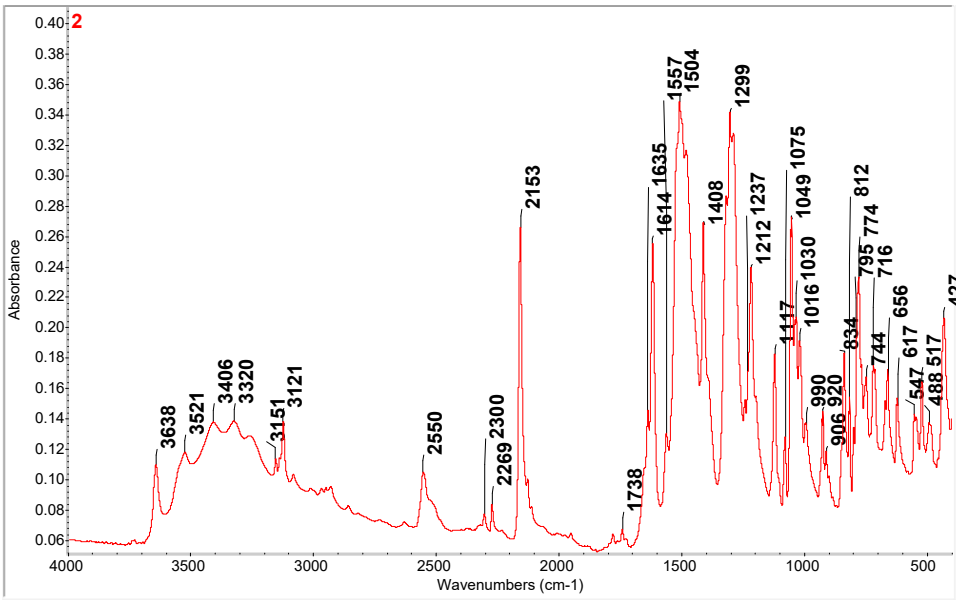

Fig. S2. FTIR spectrum of **2**.

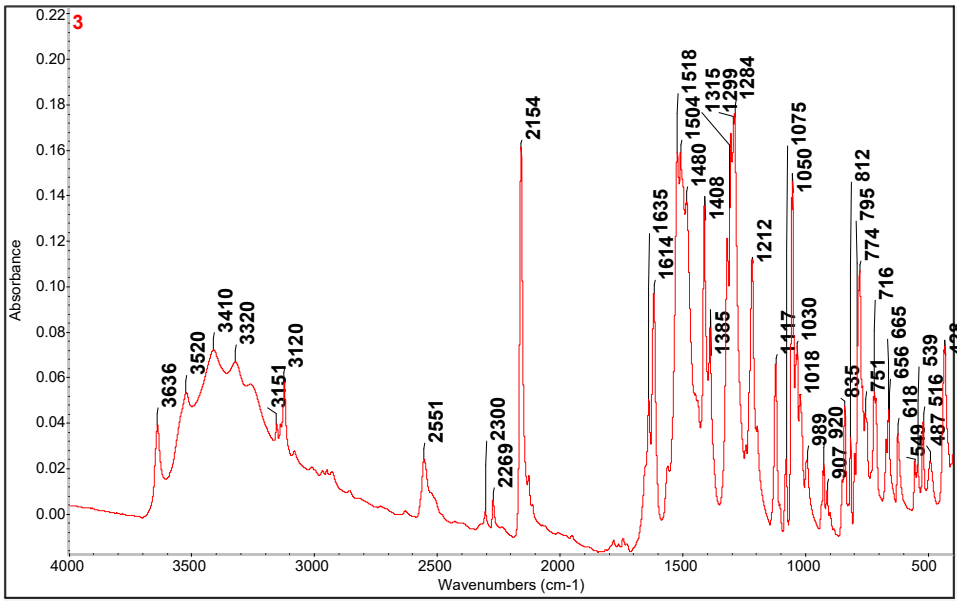

Fig. S3. FTIR spectrum of **3**

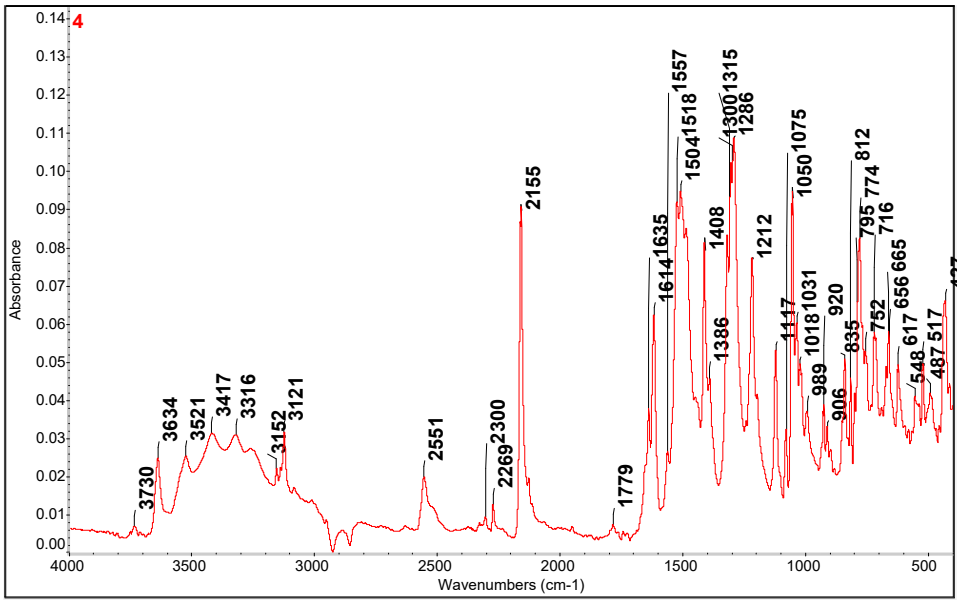

Fig. S4. FTIR spectrum of **4**.

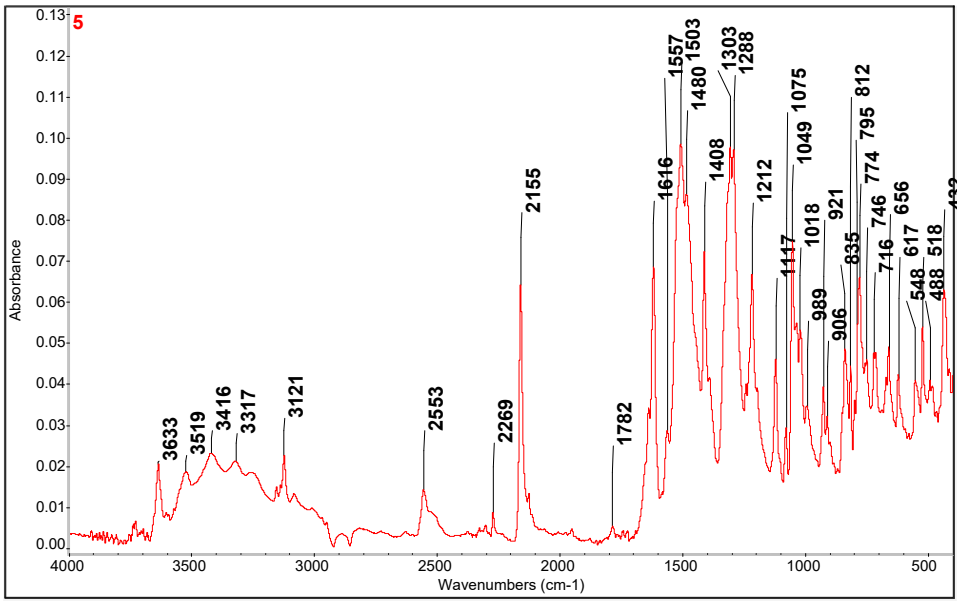

Fig. S5. FTIR spectrum of **5**.

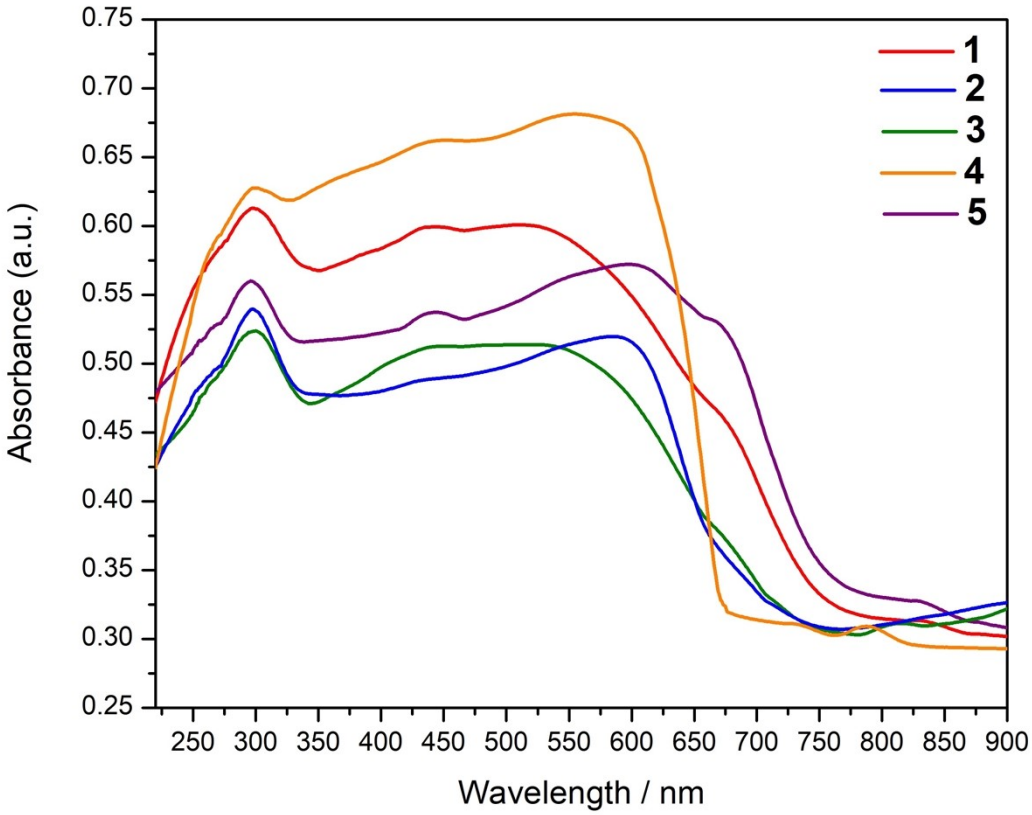

Fig. S6. UV-Vis spectra for **1-5**

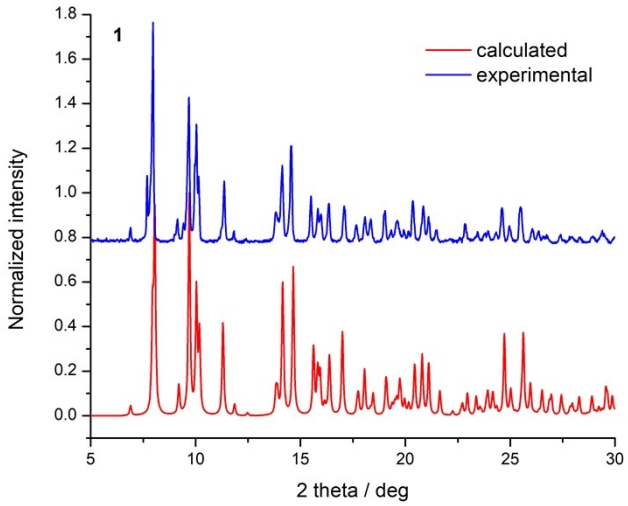

Fig. S7. Experimental and calculated powder X-ray diffractograms at room temperature for **1**.

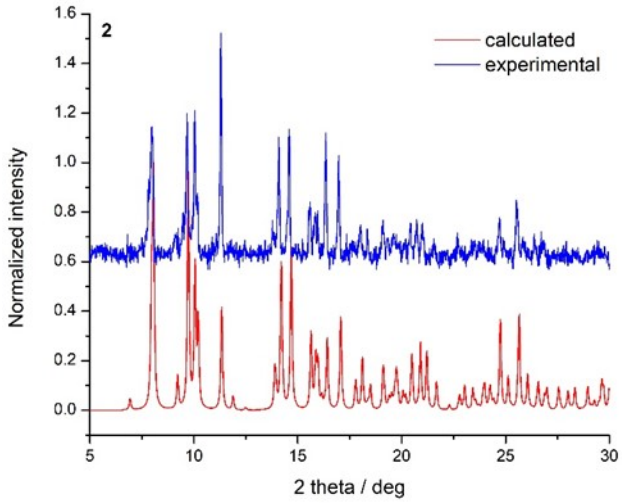

Fig. S8. Experimental and calculated powder X-ray diffractograms at room temperature for **2**.

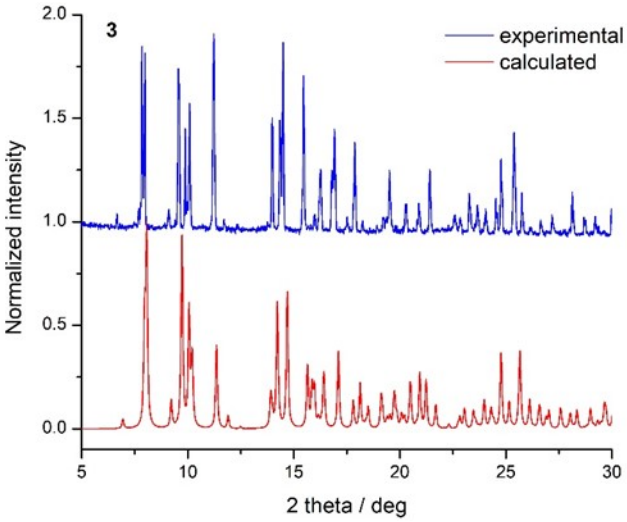

Fig. S9. Experimental and calculated powder X-ray diffractograms at room temperature for **3**.

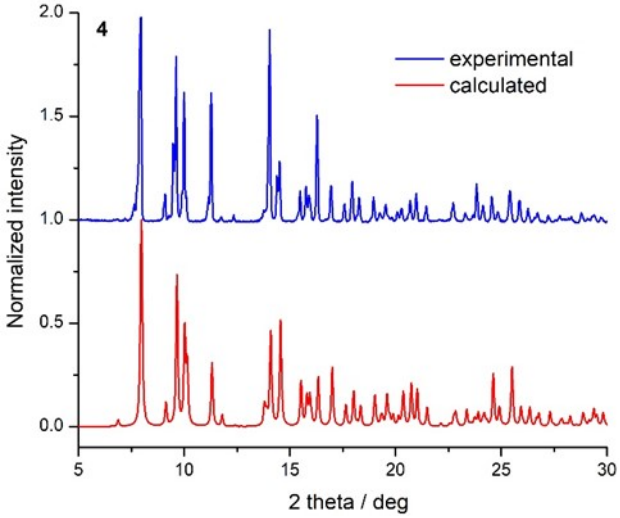

Fig. S10. Experimental and calculated powder X-ray diffractograms at room temperature for **4**.

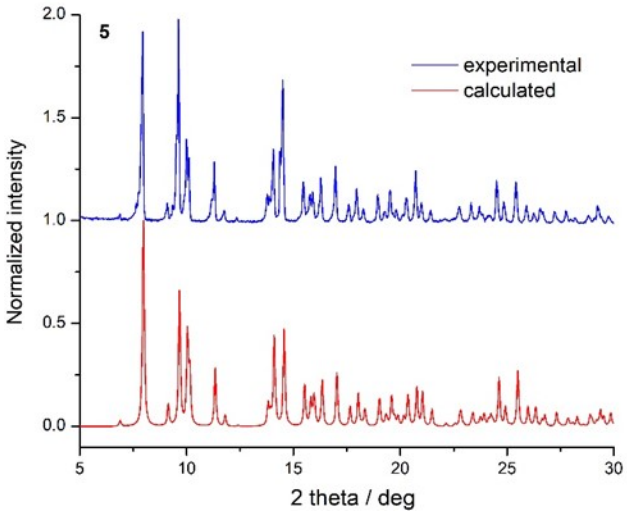

Fig. S11. Experimental and calculated powder X-ray diffractograms at room temperature for **5**.

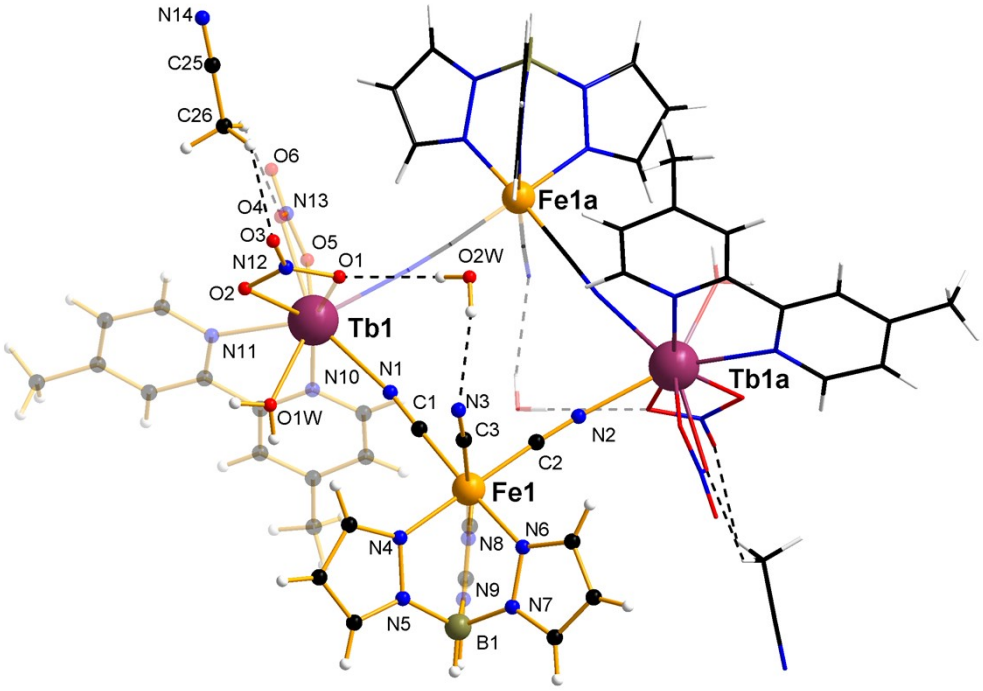

(a)

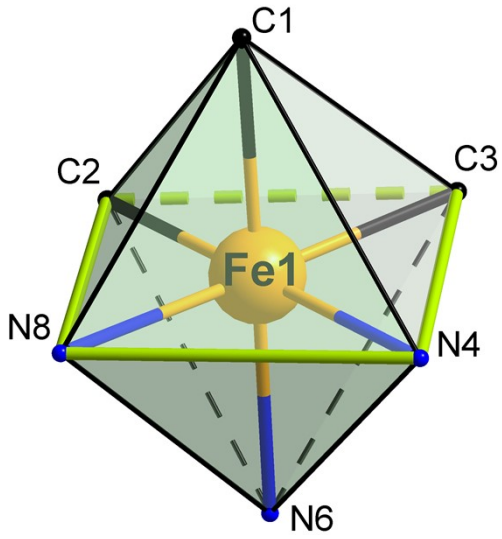

(b)

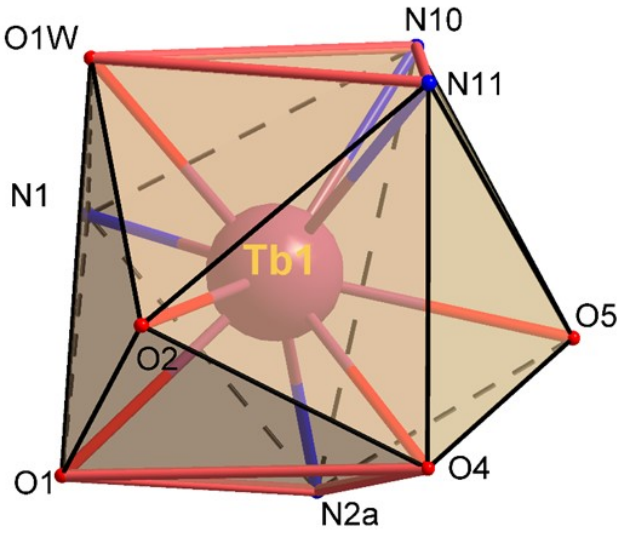

(c)

Fig. S12. View of the square-shaped cyano-bridged heterometallic unit in **2** together with the atom labelling scheme (the fragments generated by the inversion symmetry operation is represented as wires and sticks, whereas the intramolecular H-bonds established between water and acetonitrile solvent molecules and nitrate/terminal CN^- ligands of the square are represented as black dotted lines. (b) The octahedral surrounding of Fe^{III} ion. (c) Distorted tricapped trigonal prism geometry of Tb^{III} ion. [symmetry code: (*a*) = 1−*x*, 1−*y*, 2−*z*]

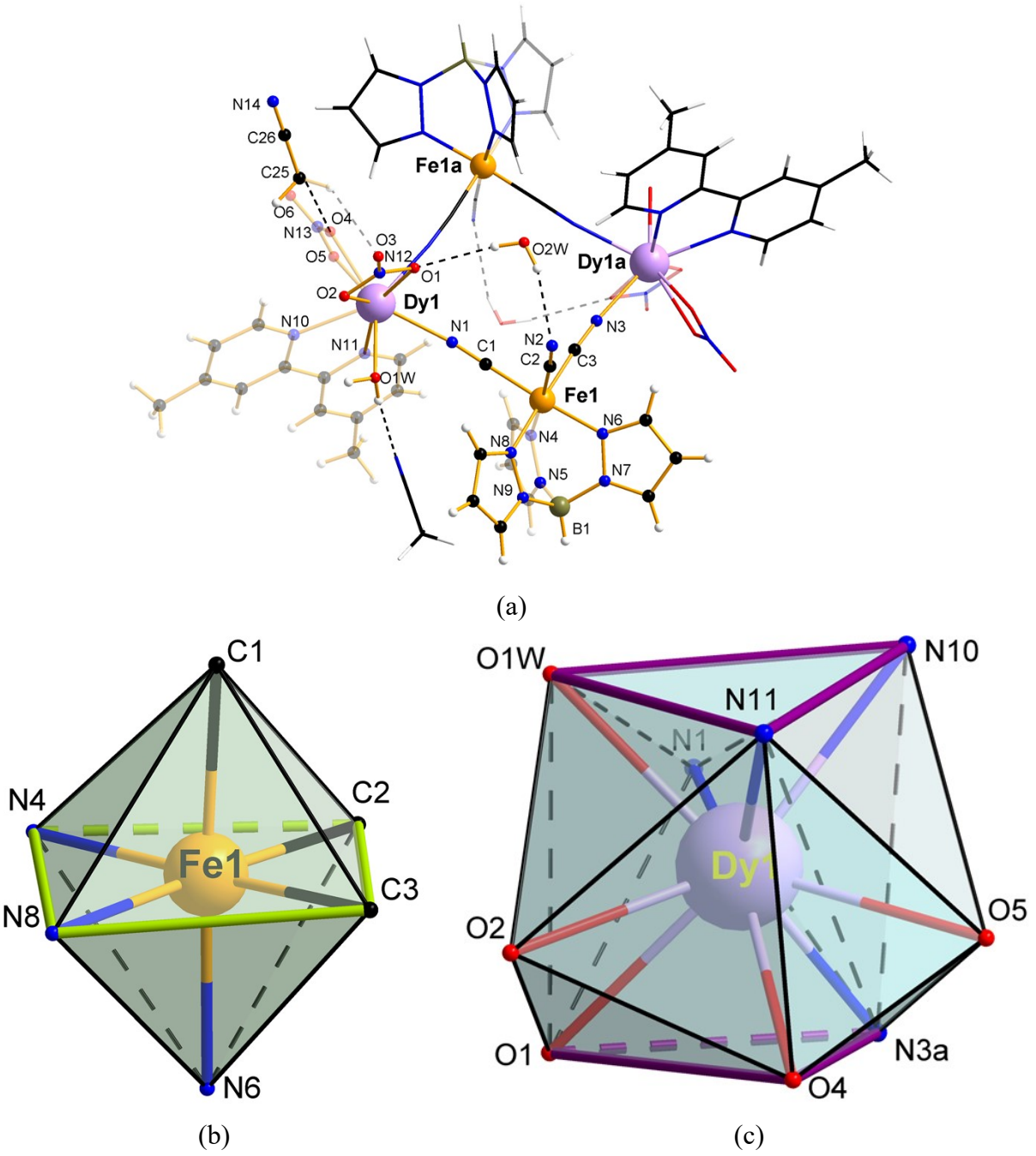

Fig. S13. View of the square-shaped cyano-bridged heterometallic unit in **3** together with the atom labelling scheme (the molecular fragment generated by the inversion symmetry operation is represented as wires and sticks and the intramolecular H-bonds established between water and acetonitrile solvent molecules and nitrate/terminal CN^- ligands of the square are represented as black dotted lines. (b) The octahedral surrounding of Fe^{III} ion. (c) Distorted tricapped trigonal prism geometry of Dy^{III} ion. [symmetry code: (*a*) = 1−*x*, 1−*y*, 1−*z*].

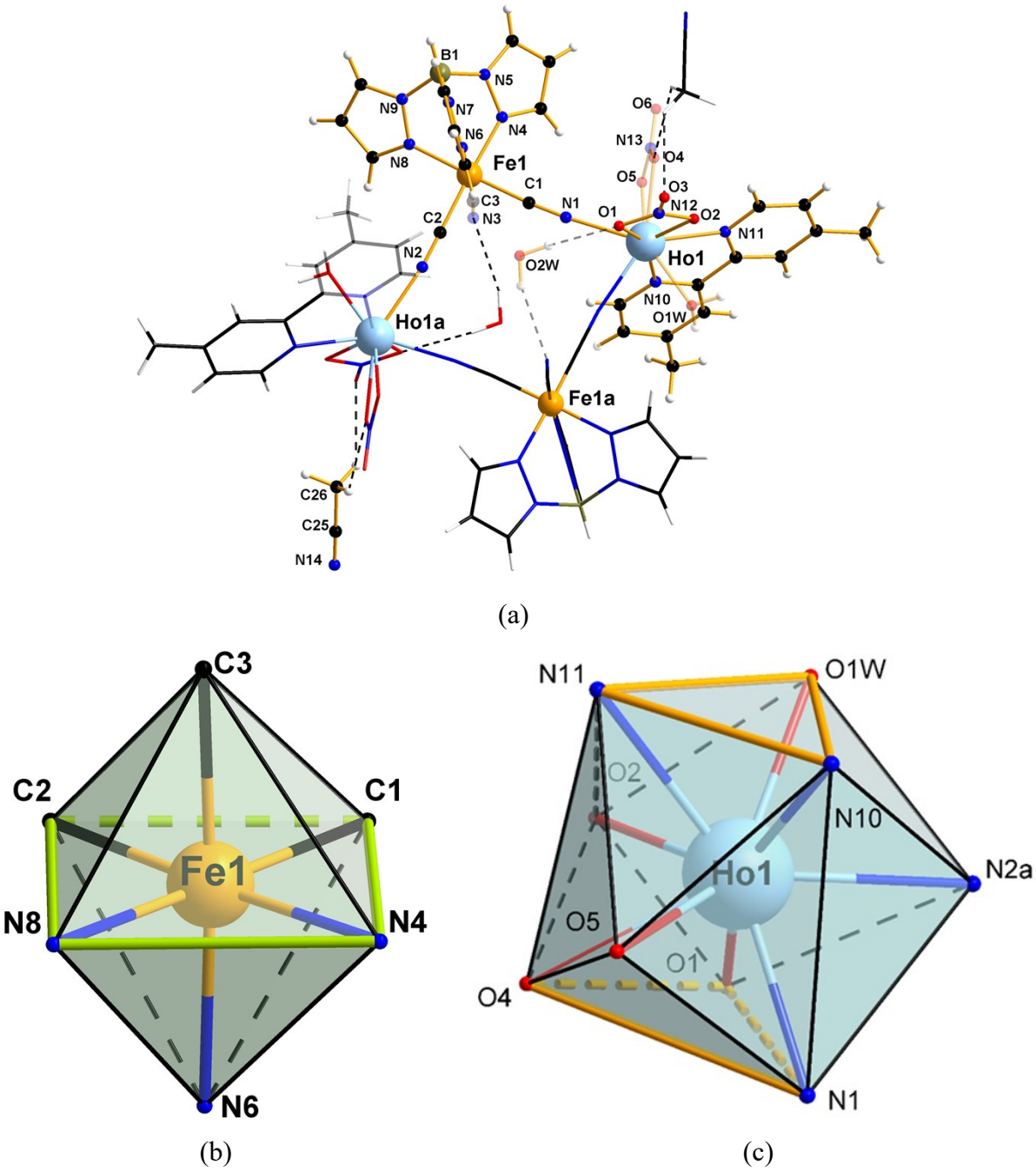

Fig. S14. View of the square-shaped cyano-bridged heterometallic unit in **4** together with the atom labelling scheme (the molecular fragment generated by the inversion symmetry operation is represented as wires and sticks and the intramolecular H-bonds established between water and acetonitrile solvent molecules and nitrate/terminal CN^- ligands of the square are represented as black dotted lines. (b) The octahedral surrounding of Fe^{III} ion. (c) Distorted tricapped trigonal prism geometry of Ho^{III} ion. [symmetry code: (*a*) = 1−*x*, 1−*y*, 1−*z*].

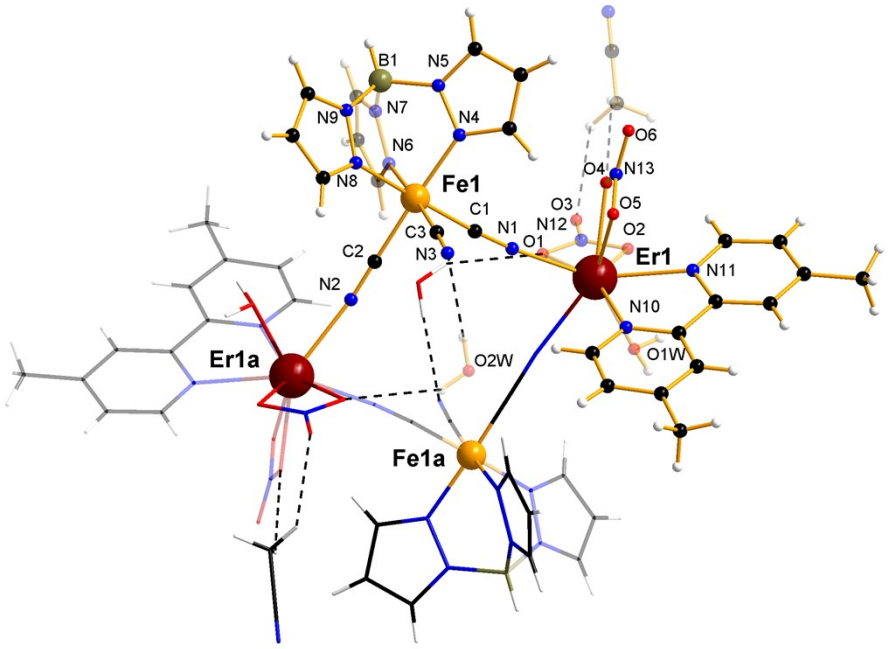

(a)

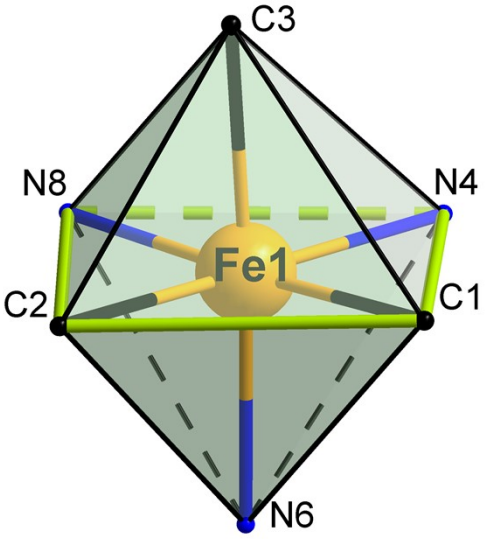

(b)

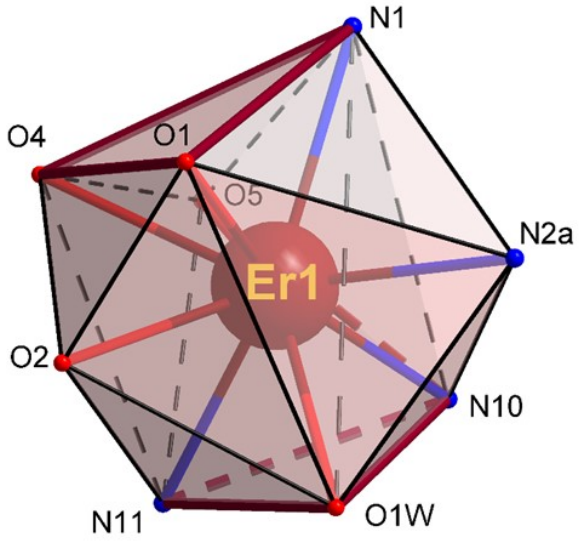

(c)

Fig. S15. View of the square-shaped cyano-bridged heterometallic unit in **5** together with the atom labelling scheme (the molecular fragment generated by the inversion symmetry operation is represented as wires and sticks and the intramolecular H-bonds established between water and acetonitrile solvent molecules and nitrate/terminal CN^- ligands of the square are represented as black dotted lines. (b) The octahedral surrounding of Fe^{III} ion. (c) Distorted tricapped trigonal prism geometry of Er^{III} ion. [symmetry code: (*a*) = 1−*x*, 1−*y*, 1−*z*].

Table S1. Bond Lengths (Å) of the environments of the iron(III) and lanthanide(III) ions in **1**-**5** [Ln = Gd (**1**), Tb (**2**), Dy (**3**), Ho(**4**), Er (**5**)]

	1	**2**	**3**	**4**	**5**
Fe1-N4	1.998(3)	1.994(3)	1.971(3)	1.972(4)	1.975(3)
Fe1-N6	1.971(3)	1.972(3)	1.974(3)	1.976(4)	1.974(3)
Fe1-N8	1.970(2)	1.968(3)	1.997(3)	1.996(4)	1.998(3)
Fe1-C1	1.914(3)	1.927(4)	1.922(4)	1.927(6)	1.931(4)
Fe1-C2	1.936(4)	1.921(4)	1.941(4)	1.933(5)	1.929(4)
Fe1-C3	1.924(3)	1.935(5)	1.923(4)	1.931(5)	1.934(4)
Ln1-N1	2.454(3)	2.449(3)	2.440(3)	2.409(5)	2.403(3)
Ln1-N2/N3a*	2.466(3)	2.439(3)	2.422(3)	2.437(4)	2.435(3)
Ln1-N10	2.549(2)	2.467(3)	2.515(3)	2.448(4)	2.427(3)
Ln1-N11	2.486(3)	2.528(3)	2.454(3)	2.514(4)	2.503(3)
Ln1-O1	2.483(2)	2.479(3)	2.508(3)	2.451(3)	2.441(2)
Ln1-O2	2.502(2)	2.480(3)	2.433(3)	2.469(3)	2.466(2)
Ln1-O4	2.522(2)	2.440(3)	2.470(3)	2.416(3)	2.406(2)
Ln1-O5	2.462(2)	2.512(3)	2.467(2)	2.516(3)	2.512(2)
Ln1-O1W	2.412(2)	2.386(3)	2.380(2)	2.384(3)	2.368(2)

* symmetry code *a* = 1-*x*, 1-*y*, 1-*z* (**1**, **3**, **4** and **5**) and *a* = 1-*x*, 1-*y*, 2-*z* (**2**)

Table S2. Bond Angles (°) of the environments of the iron(III) and lanthanide(III) ions in **1**-**5** [Ln = Gd (**1**), Tb (**2**), Dy (**3**), Ho (**4**), Er (**5**)]

	1	**2**	**3**	**4**	**5**
N4-Fe1-N6	87.61(11)	88.28(12)	89.55(13)	89.20(16)	89.26(12)
N4-Fe1-N8	88.36(10)	87.68(13)	87.68(12)	88.41(17)	88.53(11)
N6-Fe1-N8	89.29(10)	89.60(13)	88.42(12)	87.67(17)	87.68(12)
Fe1-C1-N1	176.1(3)	177.9(4)	178.5(3)	175.3(5)	175.9(3)
Fe1-C2-N2	177.1(3)	175.8(4)	176.5(4)	178.5(5)	178.6(3)
Fe1-C3-N3	178.3(3)	177.1(3)	175.6(4)	177.0(5)	177.4(4)
N4-Fe1-C1	177.70(12)	91.76(13)	92.10(14)	89.61(19)	89.57(13)
N4-Fe1-C2	177.10(12)	177.61(15)	176.80(15)	177.5(2)	177.61(13))
N4-Fe1-C3	93.01(12)	89.92(15)	93.75(14)	92.50(19)	92.63(14)
N6-Fe1-C1	94.03(12)	176.85(13)	176.77(15)	94.1(2)	94.10(14)
N6-Fe1-C2	92.08(12)	90.05(14)	92.68(15)	92.24(18)	92.11(13)
N6-Fe1-C3	176.54(12)	92.85(15)	89.88(14)	176.7(2)	176.59(14)
N8-Fe1-C1	90.04(12)	91.78(15)	94.41(14)	177.31(17)	177.38(13)
N8-Fe1-C2	94.25(11)	94.01(15)	90.09(14)	93.71(19)	93.48(13)
N8-Fe1-C3	89.87(12)	176.52(13)	177.77(15)	89.5(2)	89.52(14)
C1-Fe1-C2	88.57(14)	87.03(15)	85.78(16)	88.2(2)	88.38(14)
C1-Fe1-C3	87.32(13)	85.90(16)	87.25(15)	88.8(2)	88.77(16)
C2-Fe1-C3	85.74(13)	88.46(17)	88.55(16)	86.2(2)	86.11(15)
N10-Ln1-N11	64.68(8)	65.31(10)	65.73(10)	65.86(14)	66.22(10)
Ln1-N1-C1	173.0(3)	168.8(3)	169.3(3)	175.1(4)	174.2(3)
Ln1-N2a/N3a-C3a*	168.7(3)	173.6(3)	174.3(3)	171.3(4)	171.0(3)
O1-Ln1-O2	51.43(7)	51.53(8)	51.74(8)	52.66(12)	52.31(8)
O1-Ln1-O1W	69.13(8)	89.95(9)	142.00(9)	90.47(12)	90.72(9)
O1-Ln1-N1	120.97(8)	81.37(10)	128.51(9)	76.78(14)	76.90(10)
O1-Ln1-N2/N3	115.24(8)	75.43(10)	70.59(10)	80.32(13)	80.28(9)
O1-Ln1-N10	78.17(8)	159.98(9)	70.75(9)	159.98(13)	159.72(9)
O1-Ln1-N11	137.81(8)	129.51(9)	71.43(9)	129.79(13)	129.72(9)
O1-Ln1-O4	115.48(7)	78.45(9)	123.69(9)	77.93(12)	77.73(9)
O1-Ln1-O5	68.33(8)	123.62(9)	115.61(9)	123.22(12)	123.26(9)
O2-Ln1-O1W	89.65(7)	69.13(9)	133.52(9)	68.71(12)	69.04(8)
O2-Ln1-O4	123.47(7)	68.36(9)	78.63(9)	68.38(12)	68.27(9)
O2-Ln1-O5	78.64(8)	115.72(9)	68.34(9)	114.88(12)	115.06(9)
O2-Ln1-N1	75.42(8)	114.78(10)	149.49(10)	123.70(13)	123.65(10)
O2-Ln1-N2a/N3a*	81.93(8)	121.06(10)	78.60(10)	114.07(12)	113.87(9)
O2-Ln1-N10	129.43(8)	138.32(9)	79.37(10)	138.26(13)	138.76(9)
O2-Ln1-N11	160.44(8)	78.16(9)	120.58(9)	77.37(12)	77.66(9)

O4-Ln1-O5	51.38(7)	51.72(9)	52.11(9)	51.51(11)	51.74(9)
O4-Ln1-O1W	142.30(7)	133.27(9)	90.03(9)	133.23(13)	133.33(9)
O4-Ln1-N1	71.06(8)	149.58(9)	80.84(9)	79.37(14)	79.69(10)
O4-Ln1-N2a/N3a*	150.09(8)	78.65(9)	75.58(10)	148.82(14)	148.63(10)
O4-Ln1-N10	70.95(8)	120.39(10)	129.86(9)	120.42(12)	120.82(9)
O4-Ln1-N11	71.52(8)	79.45(9)	159.40(10)	79.60(13)	79.59(9)
O5-Ln1-O1W	133.26(8)	141.92(9)	69.26(9)	141.43(11)	141.23(9)
O5-Ln1-N1	78.89(8)	128.27(10)	114.68(9)	70.73(13)	70.90(9)
O5-Ln1-N2a/N3a*	150.10(8)	70.92(10)	121.59(10)	129.91(13)	129.86(10)
O5-Ln1-N10	79.31(8)	71.38(10)	77.92(9)	71.15(12)	71.25(9)
O5-Ln1-N11	119.95(8)	70.88(9)	138.46(10)	70.16(12)	70.08(9)
O1W-Ln1-N1	141.60(8)	68.73(9)	68.39(10)	142.07(13)	141.79(9)
O1W-Ln1-N2/N3a*	68.57(8)	141.95(10)	141.95(10)	68.57(13)	68.59(9)
O1W-Ln1-N10	73.92(8)	81.51(10)	74.02(9)	82.17(12)	81.89(9)
O1W-Ln1-N11	81.50(8)	73.73(10)	81.54(9)	73.74(12)	73.74(8)
N1-Ln1-N10	141.95(9)	78.66(10)	131.08(10)	97.71(15)	97.33(11)
N1-Ln1-N11	100.93(9)	130.89(10)	78.58(10)	140.70(13)	140.77(9)
N2a/3a-Ln1-N10*	78.61(8)	100.35(11)	141.29(10)	79.66(13)	79.43(10)
N2a/3a-Ln1-N11*	130.48(8)	141.74(10)	99.68(11)	131.57(13)	131.77(9)
N1-Ln1-N2a/N3a*	74.34(9)	74.38(10)	74.56(10)	74.08(14)	73.71(10)

* symmetry code *a* = 1-*x*, 1-*y*, 1-*z* (**1**, **3**, **4** and **5**) and *a* = 1-*x*, 1-*y*, 2-*z* (**2**)

Table S3. Summary of the SHAPE analysis for the the six-coordinated [$Fe^{III}C_3N_3$] and nine-coordinated [$Ln^{III}N_4O_5$] fragment in **1-5** [Ln = Gd (**1**), Tb (**2**), Dy (**3**), Ho (**4**), Er (**5**)].

Compounds	**1**	**2**	**3**	**4**	**5**
CN = 6[a]			Fe^{III}		
HP-6	32.368	32.394	32.427	32.467	32.403
PPY-6	28.259	28.178	28.301	28.336	28.356
OC-6	**0.153**	**0.156**	**0.148**	**0.129**	**0.126**
TPR-6	14.732	14.678	14.838	14.841	14.858
JPPY-6	32.042	31.960	32.088	32.142	32.150
CN = 9[b]	Gd^{III}	Tb^{III}	Dy^{III}	Ho^{III}	Er^{III}
EP-9	35.345	35.387	35.429	35.801	35.848
OPY-9	22.156	22.174	22.123	22.343	22.416
HBPY-9	16.985	17.035	17.169	17.465	17.528
JTC-9	15.308	15.282	15.199	14.985	14.913
JCCU-9	8.649	8.736	8.816	8.945	8.987
CCU-9	7.276	7.419	7.479	7.651	7.717
JCSAPR-9	3.233	3.171	3.150	2.965	2.908
CSAPR-9	2.343	2.322	2.254	2.109	2.063
JTCTPR-9	3.566	3.446	3.351	3.216	3.158
TCTPR-9	**1.900**	**1.829**	**1.774**	**1.744**	**1.738**
JTDIC-9	11.554	11.596	11.714	11.775	11.775
HH-9	11.136	11.160	11.120	11.106	11.102
MFF-9	2.288	2.205	2.132	2.080	2.038

The listed values correspond to the deviation between the ideal and real coordination polyhedraw, the lowest values being given in bold. [a] PPY-6, C_{5v} Pentagonal pyramid; OC-6, O_h Octahedron; TPR-6, D_{3h} Trigonal prism; JPPY-5, C_{5v} Johnson pentagonal pyramid (J2);[b]EP-9, D_{9h}, enneagon; OPY-9, C_{8v}, octagonal pyramid; HBPY-9, D_{7h}, heptagonal bipyramid; JTC-9, C_{3v}, Johnson triangular cupola J3; JCCU-9, C_{4v}, capped cube J8; CCU-9, C_{4v}, spherical-relaxed capped cube; JCSAPR-9, C_{4v}, capped square antiprism; CSAPR-9, C_{4v}, spherical capped square antiprism; JTCTPR-9, D_{3h}, tricapped trigonal prism J51; TCTPR-9, D_{3h}, spherical tricapped trigonal prism; JTDIC-9, C_{3v}, tridiminished icosahedron; HH-9, C_{2v}, hula-hoop; MFF-9, C_s, muffin.

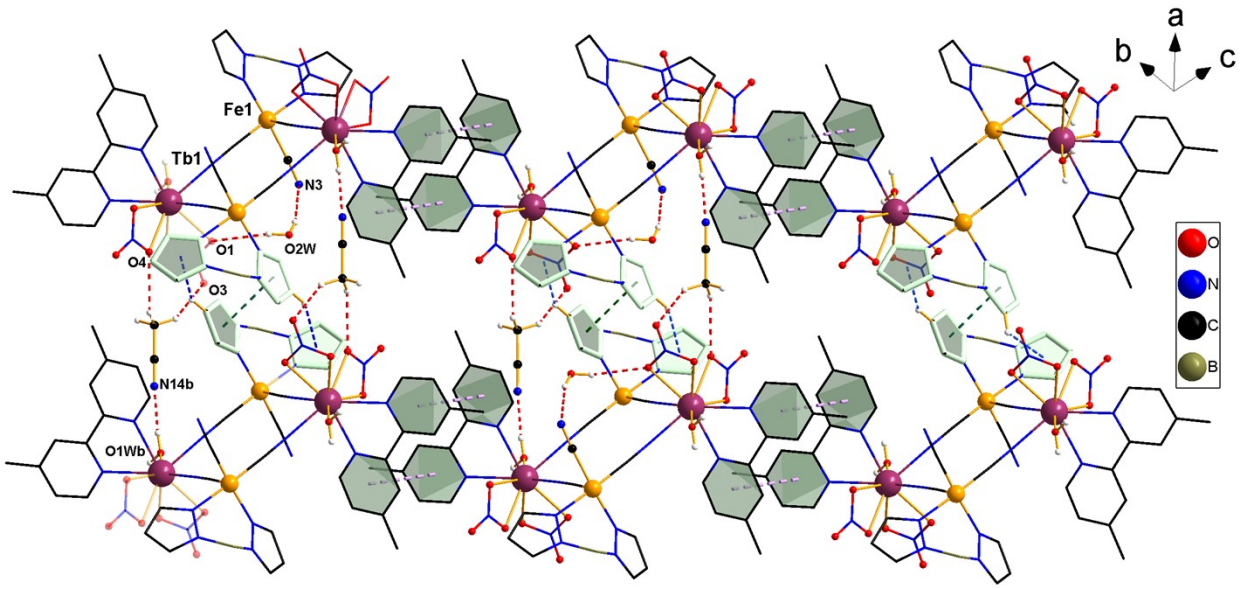

Fig. S16. View of crystal packing for **2** showing the layers formed by the interplaying of H-bonds (O···H-O and N···H-O type) and C-H···π and the offset π···π stacking interactions established between peripheral dmbipy ligands, $(\pi\cdots\pi)_{dmbipy}$ as well as between two pyrazolyl rings of $\{HB(pz)_3\}^-$ ligands [one pyrazolyl ring was removed for the sake of clarity, symmmetry code (*b)* = -1+*x*, *y*, *z*].

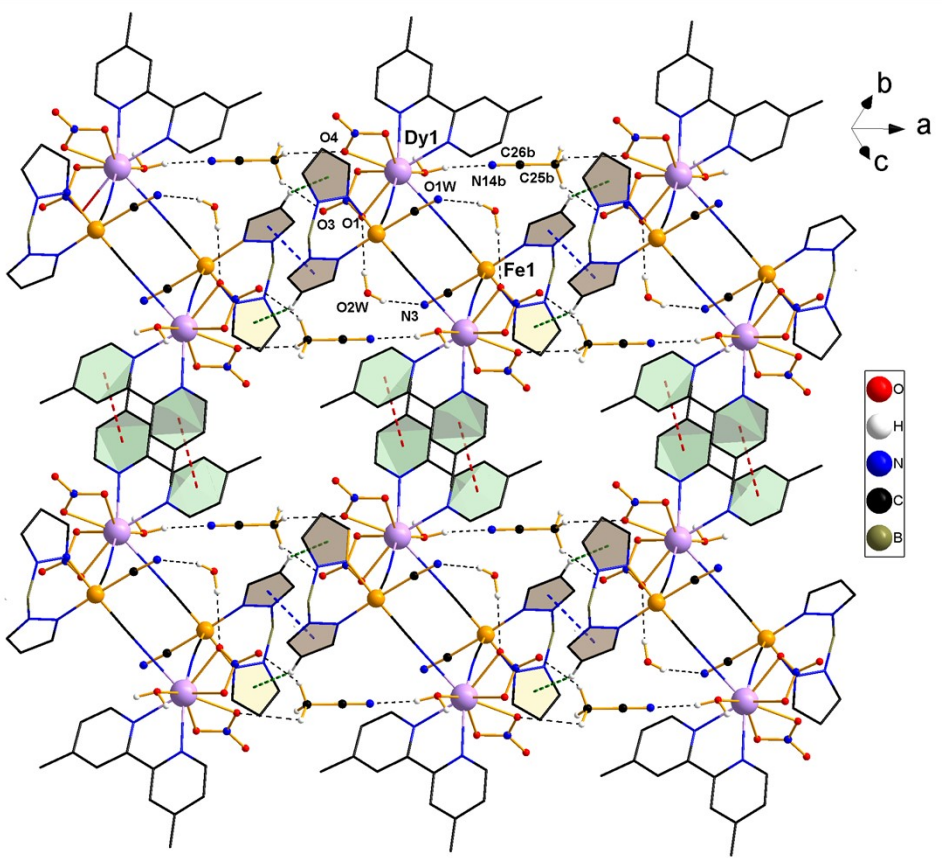

Fig. S17. View of crystal packing in **3** showing the layers formed by O···H-O and N···H-O type H-bonds, C-H···π and π···π stacking interactions established between the pyrazolyl rings for **3** (dmbpy ligands, one pyrazolyl ring and the terminal cyanide ligand were removed for the sake of clarity), 3.39 Å/17.46º (π···π) and 2.81 Å (C-H···π), symmmetry code (*b)* = 1+*x*, *y*, *z*.

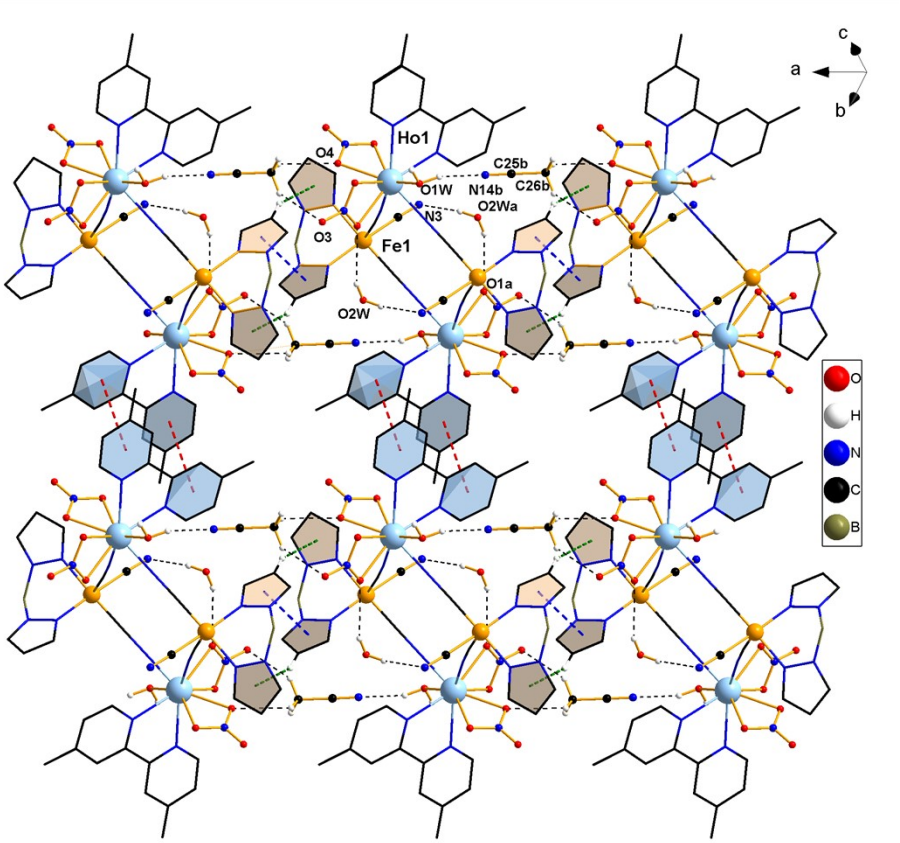

Fig S18. View of crystal packing showing the layers formed through offset π···π stacking interactions for **4** established between pyridine and pyrazolyl rings of dmbipy and $HB(pz)_3$, respectively, ligands (two pyrazolyl ring, the terminal cyanide, aqua and nitrate ligands as well as crystallization water and acetonitrile molecules were removed for the sake of clarity). The average centroid-centroid distance is *ca*. 3.90 Å (pyridine-pyridine rings of dmbipy ligand), whereas the angles between the normal to the ring and the centroid−centroid vector are of *ca*. 23.80 and 24.84°. Symmmetry codes: (a) = 1-*x*, 1-*y*, 1-*z*; (*b)* = 1+*x*, *y*, *z*.

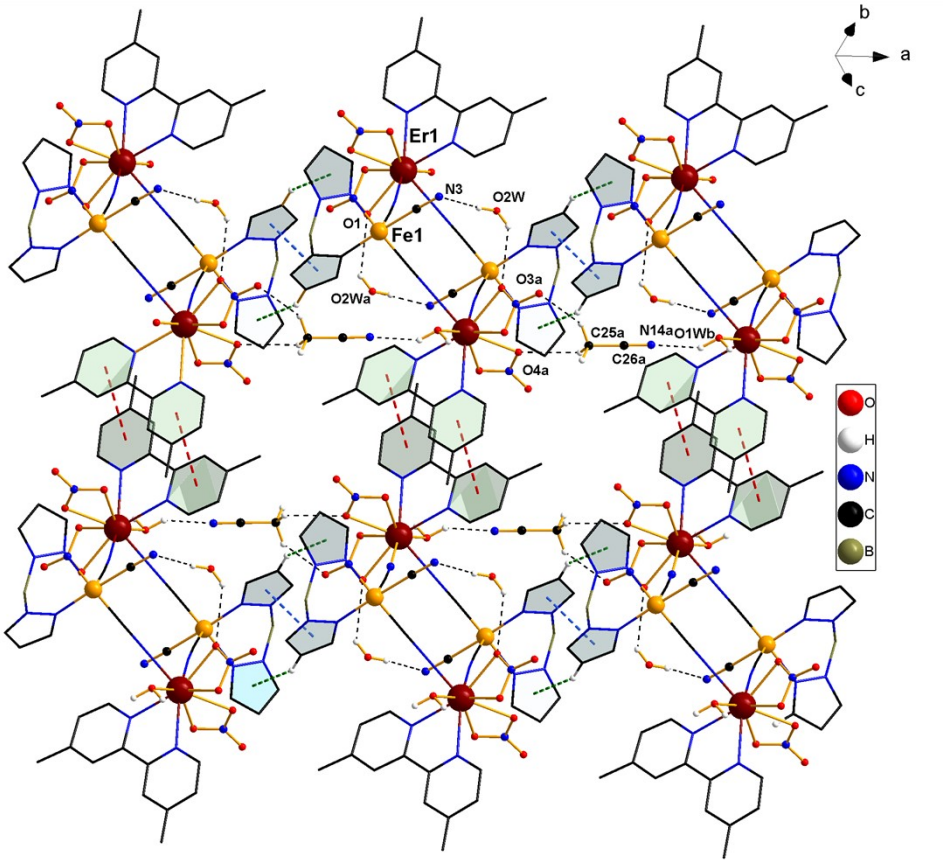

Fig. S19. View of crystal packing in *ac* crystallographic plane showing the layers formed by O···H-O and N···H-O type H-bonds, C-H···π and π···π stacking interactions established between the pyrazolyl rings for **5** (dmbpy ligands, one pyrazolyl ring and the terminal cyanide ligand were removed for the sake of clarity): 3.64 Å/14.09º (π···π) and 2.76 Å (C-H···π). Symmmetry codes: (a) = 1-*x*, 1-*y*, 1-*z*, (*b*) = 1+*x*, *y*, *z*.

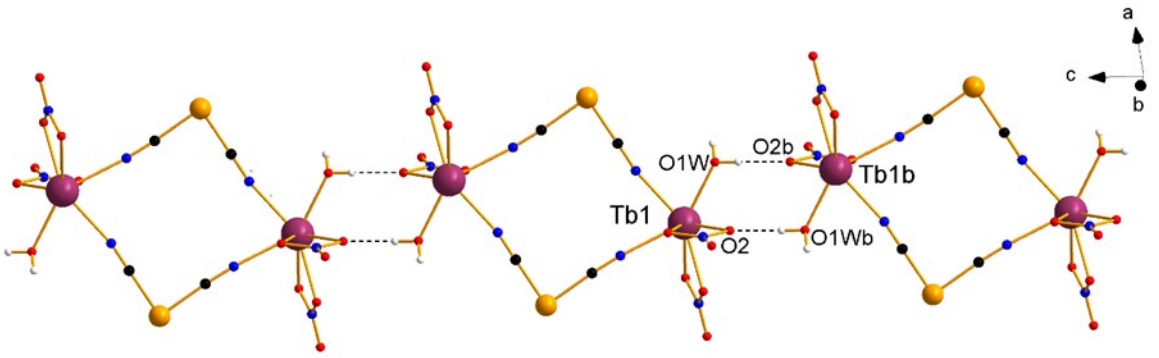

Fig. S20. View along *c* crystallographic axis showing the H-bonds established between peripheral via aqua (O1W) and nitrate ligands (O2) (black dotted lines) in **2**. The $\{HB(pz)_3\}^-$, dmbipy and the terminal cyanide ligands, as well as the crystallization water and acetonitrile molecules were omitted for the sake of clarity [symmetry code: (*c*) = 1-*x*, 1-*y*, 1-*z*].

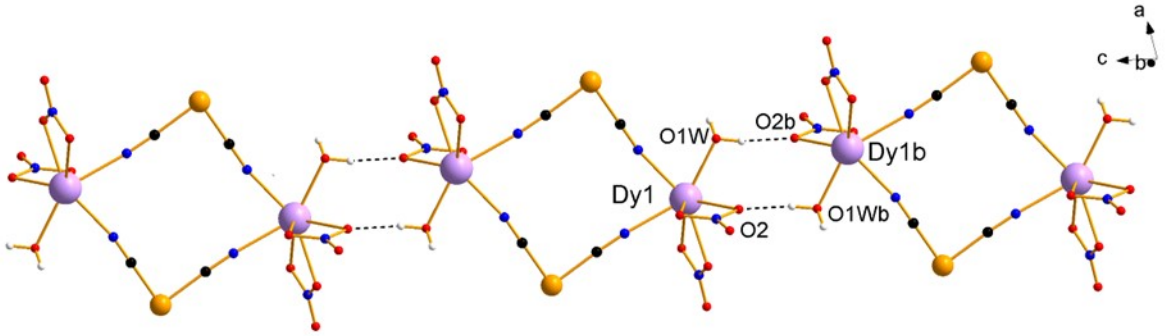

Fig. S21. View along *c* crystallographic axis showing the H-bonds established between peripheral via aqua (O1W) and nitrate ligands (O2) (black dotted lines) in **3**. The $\{HB(pz)_3\}^-$, dmbipy and the terminal cyanide ligands, as well as the crystallization water and acetonitrile molecules were omitted for the sake of clarity [symmetry code: (*c*) = 1-*x*, 1-*y*, 2-*z*].

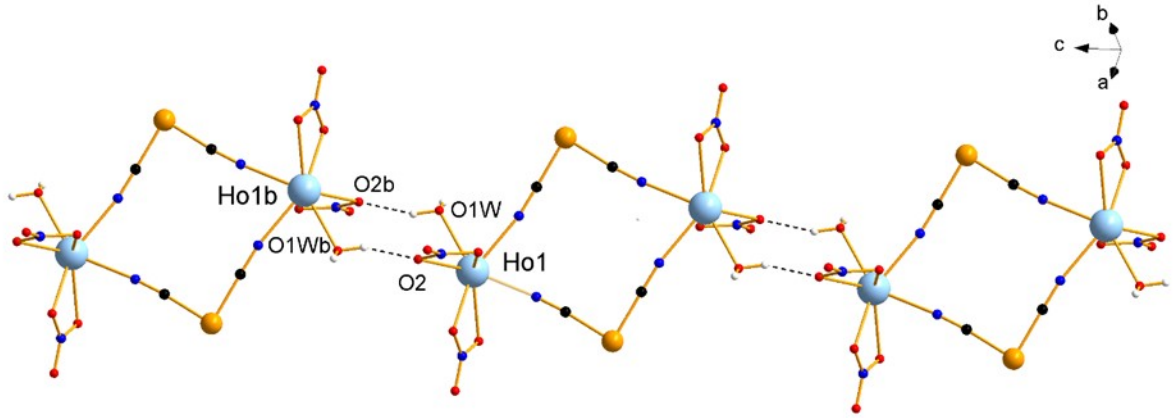

Fig. S22. View along *c* crystallographic axis showing the H-bonds established between peripheral via aqua (O1W) and nitrate ligands (O2) (black dotted lines) in **4**. The $\{HB(pz)_3\}^-$, dmbipy and the terminal cyanide ligands, as well as the crystallization water and acetonitrile molecules were omitted for the sake of clarity [symmetry code: (*c*) = 1-*x*, 1-*y*, 2-*z*]

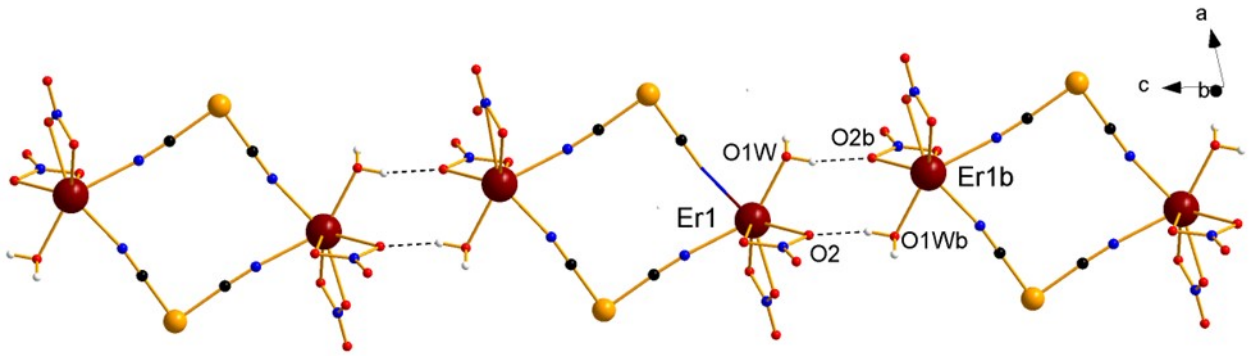

Fig. S23. View along *c* crystallographic axis showing the H-bonds established between peripheral via aqua (O1W) and nitrate ligands (O2) (black dotted lines) in **5**. The $\{HB(pz)_3\}^-$, dmbipy and the terminal cyanide ligands, as well as the crystallization water and acetonitrile molecules were omitted for the sake of clarity [symmetry code: (*c*) = 1-*x*, 1-*y*, 2-*z*]

Table S4. Selected intermolecular contacts for **1-5***

Compound	D-H···A	D-H (Å)	H···A (Å)	D···A (Å)	Angle D-H···A
1	O2W-H2WA···N3	0.85	2.44	3.088(5)	133
	O2W-H2WA···O2^{a}	0.87	2.40	3.261(3)	174
	O1W^{b}-H1WA^{b}···O1	0.85	2.00	2.780(3)	151
	O1W^{c}-H1WA^{c}···N14	0.85	1.97	2.800(4)	165
	C25-H25A···O3	0.98	2.49	3.322(5)	142
	C25-H25C···O4	0.98	2.53	3.185(5)	124
2	O2W-H2WA···N3	0.85(5)	2.27(5)	3.094(6)	165(5)
	O2W-H2WB···O1	0.84(4)	2.44(4)	3.251(5)	161(4)
	O1W-H1WA···O2^{b}	0.84(3)	1.94(3)	2.777(4)	176(5)
	O1W-H1WB···N14	0.833(17)	1.963(18)	2.795(5)	176(4)
	C26-H26B···O3^{c}	0.96	2.49	3.320(6)	144.7
	C26-H26B···O4^{c}	0.96	2.53	3.183(5)	125.7
3	O2W-H2WA···N3	0.846(19)	2.27(3)	3.094(5)	165(5)
	O2W-H2WB···O1	0.843(19)	2.44(3)	3.250(4)	160(6)
	C(4)-H(4) ···O(2W)^{b}	0.93	2.55	3.410(5)	154.6
	O1W-H1WA···N14^{c}	0.87	1.94	2.790(5)	165
	O1W-H1WB···O2^{b}	0.87	1.96	2.783(4)	157
	C25^{c}-H25A^{c}···O3^{c}	0.96	2.49	3.310(5)	144
	C25^{c}-H25A^{c}···O4^{c}	0.96	2.52	3.181(5)	126
4	O2W-H2WA···N3	0.85	2.97	3.096(9)	-
	O2W-H2WA···O1^{a}	0.85	2.56	3.288(9)	145
	C(4)-H(4) ···O(2W)^{b}	0.89	1.95	2.810(7)	164
	O1W^{c}-H1WA^{c}···N14^{c}	0.85	2.01	2.801(5)	155
	O1W^{c}-H1WB^{c}···O2^{a}	0.89	1.99	2.810(5)	153
	C26^{c}-H26B^{c}···O3^{a}	0.96	2.57	3.357(8)	139
	C26^{c}-H26B^{c}···O4^{a}	0.96	2.60	3.197(8)	121
5	O2W-H2WA···N3	0.85	2.47	3.103(6)	131
	O2W-H1WA···O1^{a}	0.85	2.56	3.288(8)	145
	C25-H25B···O3	0.96	2.52	3.336(6)	142.3
	C25-H25C···O4	0.96	2.59	3.218(6)	123.1

*D = donor and A = acceptor. ^{i}Symmetry code: (*a*) = 1-*x*, 1-*y*, 1-*z* (**1**, **3-5**), 1-*x*, 1-*y*, 2-*z* (**2**); (*b*) = 1+*x*, *y*, *z* (**1**, **3-5**), -1+*x*, *y*, *z* (**2**), (*c*) = 1-*x*,1-*y*, 2-*z* (**1**, **3-5**), 1-*x*,1-*y*, 1-*z* (**2**)

Table S5. Dc and ac magnetic parameters for cyano-bridged $\{Ln^{III}_2Fe^{III}_2\}$ squares

Compounds	$J_{Fe\text{-}Ln}$ (cm^{-1})	$J_{Fe\text{-}Fe'}$ (cm^{-1})	g_{Fe}	λ_{Fe} (cm^{-1})	λ_{Ln} (cm^{-1})	Δ_{Fe} (cm^{-1})	Δ_{Ln} (cm^{-1})	θ (K)	$\chi_{TIP}\times10^{-6}$ (cm^3mol^{-1})	U_{eff} (cm^{-1})	Ref.
$[Fe^{III}(htpzb)(CN)(\mu\text{-}CN)_2La^{III}(pyim)_2(NO_3)_2]_2\cdot10H_2O$[b]	-	-2.32(3)	2.198(4)	-				-0.650(7)	266(5)	-	55
$[Fe^{III}(htpzb)(CN)(\mu\text{-}CN)_2Gd^{III}(pyim)(NO_3)_2(H_2O)]_2\cdot6H_2O$[b]	-2.06(3)	-0.210(4)	2.23(1)	-				-0.450(5)	280(5)	-	55
$[Fe^{III}(htpzb)(CN)(\mu\text{-}CN)_2Tb^{III}(pyim)(NO_3)_2(H_2O)]_2\cdot2.6H_2O$[b]	-	-		-						-	55
$[Fe^{III}(htpzb)(CN)(\mu\text{-}CN)_2Dy^{III}(pyim)(NO_3)_2(H_2O)]_2\cdot4H_2O$[b]	-	-		-						-	55
$[Fe^{III}(htpzb)(CN)(\mu\text{-}CN)_2Eu^{III}(pyim)(Ph_3PO)(NO_3)_2]_2\cdot2CH_3CN$[c]	-0.042(1)	-		-395(1)	+ 289(1)	760(3)	-	-	-	-	56
$[Fe^{III}(htpzb)(CN)(\mu\text{-}CN)_2Sm^{III}(pyim)(Ph_3PO)(NO_3)_2]_2\cdot2CH_3CN$[c]	-0.098(1)	-		-385(1)	+ 218(1)	606(3)	-	-	-	-	56
$[Fe^{III}(htpzb)(CN)(\mu\text{-}CN)_2Ce^{III}(pyim)(Ph_3PO)(NO_3)_2]_2\cdot2CH_3CN$[c]	-	-0.28	2.272		600*		57.0	-0.71	1468		57
$[Fe^{III}(htpzb)(CN)(\mu\text{-}CN)_2Pr^{III}(pyim)(Ph_3PO)(NO_3)_2]_2\cdot2CH_3CN$[c]			2.322		360*		26.7		2746		57
$[Fe^{III}(htpzb)(CN)(\mu\text{-}CN)_2Nd^{III}(pyim)(Ph_3PO)(NO_3)_2]_2\cdot2CH_3CN$[c]	-1.37	-1.29	2.327		260*		71.7	-1.90	1036		57
$[Fe^{III}(htpzb)(CN)(\mu\text{-}CN)_2Gd^{III}(pyim)(Ph_3PO)(NO_3)_2]_2\cdot2CH_3CN$[c]	-2.32	-0.22	2.41		-			-0.28	1672		57
$[Fe^{III}(htpzb)(CN)(\mu\text{-}CN)_2Tb^{III}(pyim)(Ph_3PO)(NO_3)_2]_2\cdot2CH_3CN$[c]	-1.88		2.280		−570*		4.0	-1.90	2619	13–17	57
$[Fe^{III}(htpzb)(CN)(\mu\text{-}CN)_2Dy^{III}(pyim)(Ph_3PO)(NO_3)_2]_2\cdot2CH_3CN$[c]	-2.50		2.219		−380*		18.9	-0.33	2956	25–28	57
$[Fe^{III}(htpzb)(CN)(\mu\text{-}CN)_2Er^{III}(pyim)(Ph_3PO)(NO_3)_2]_2\cdot2CH_3CN$[c]	-0.13	-0.21	2.344		−680*		72.8	-0.43	2981	38–40	57

[a] bpy = 2,2'-bipyridine;
[b] htpzb = hydrotris(pyrazolyl)borate; pyim = 2-(1H-imidazol-2-yl)pyridine; κ_{Fe} = 0.862(2) for Eu^{III} and 0.852(2) for Sm^{III} derivatives; λ_{Fe} and λ_{Ln} are spin-orbit coupling parameters; Δ_{Fe} and Δ_{Ln} energy gap parameters
[c] Ph_3PO = triphenylphosphine oxide;
* fixed values

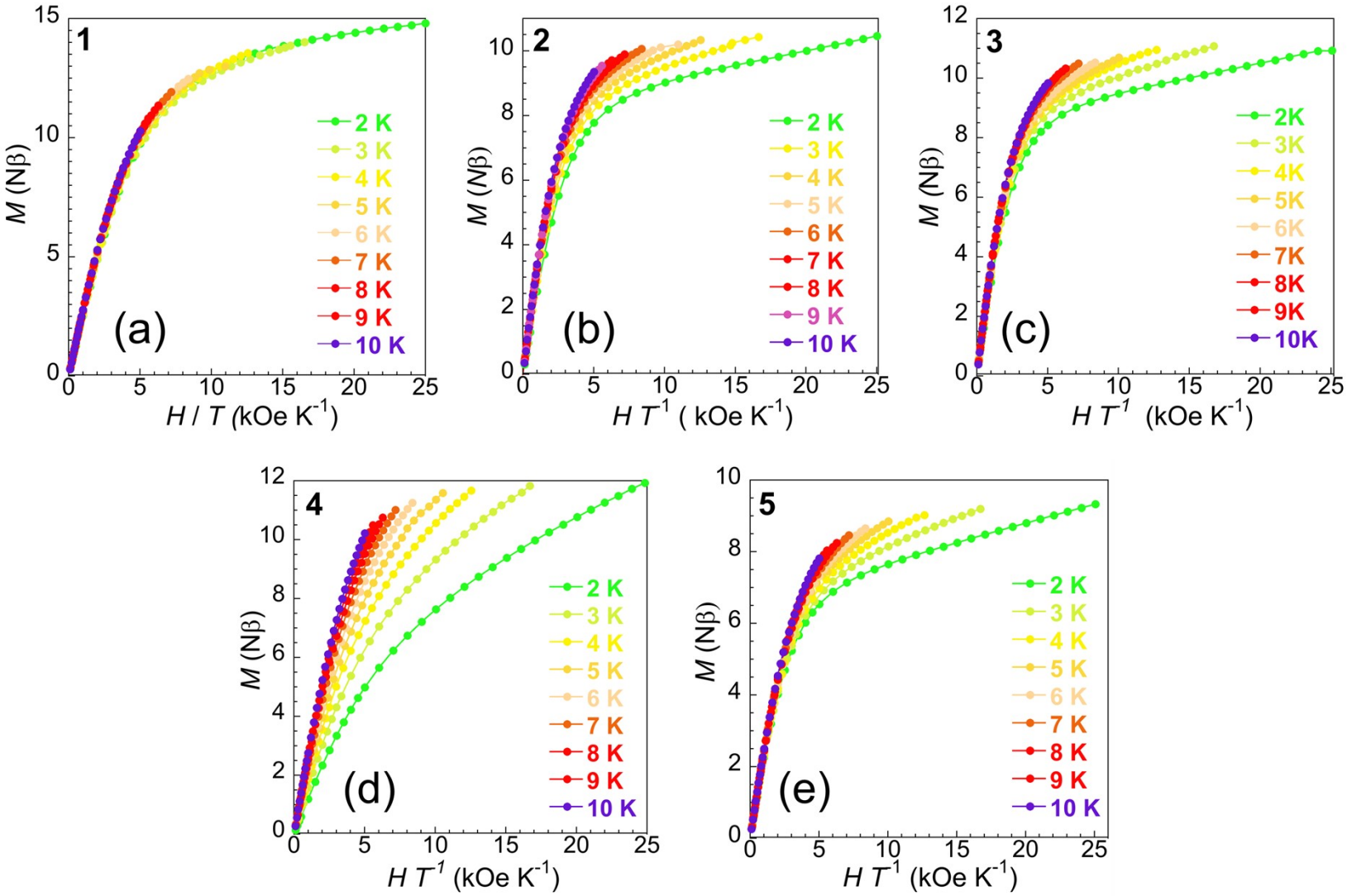

Fig. S24. The reduced field dependence of *M* for **1-5** (a-e).

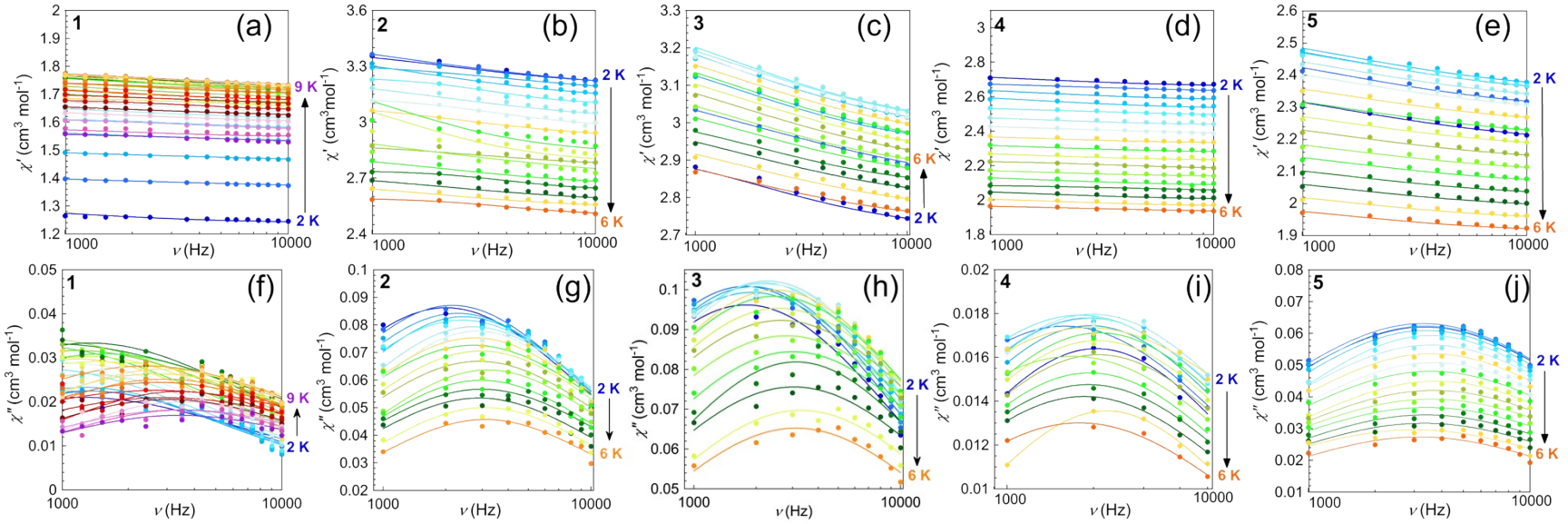

Fig. S25. Frequency dependence of χ_M' (a-e) and χ_M" (f-j) for **1-5** at ±5 Oe oscillating field in the temperature range 2.0-9.0 K (**1**, blue to violet) and 2.0-6.0 K (**2-5**) (blue to orange) and under an applied static magnetic field of 1.0 (**1**) or 0.5 T (**2**–**5**). The solid lines are the best-fit curves through the generalized Debye model (see text).

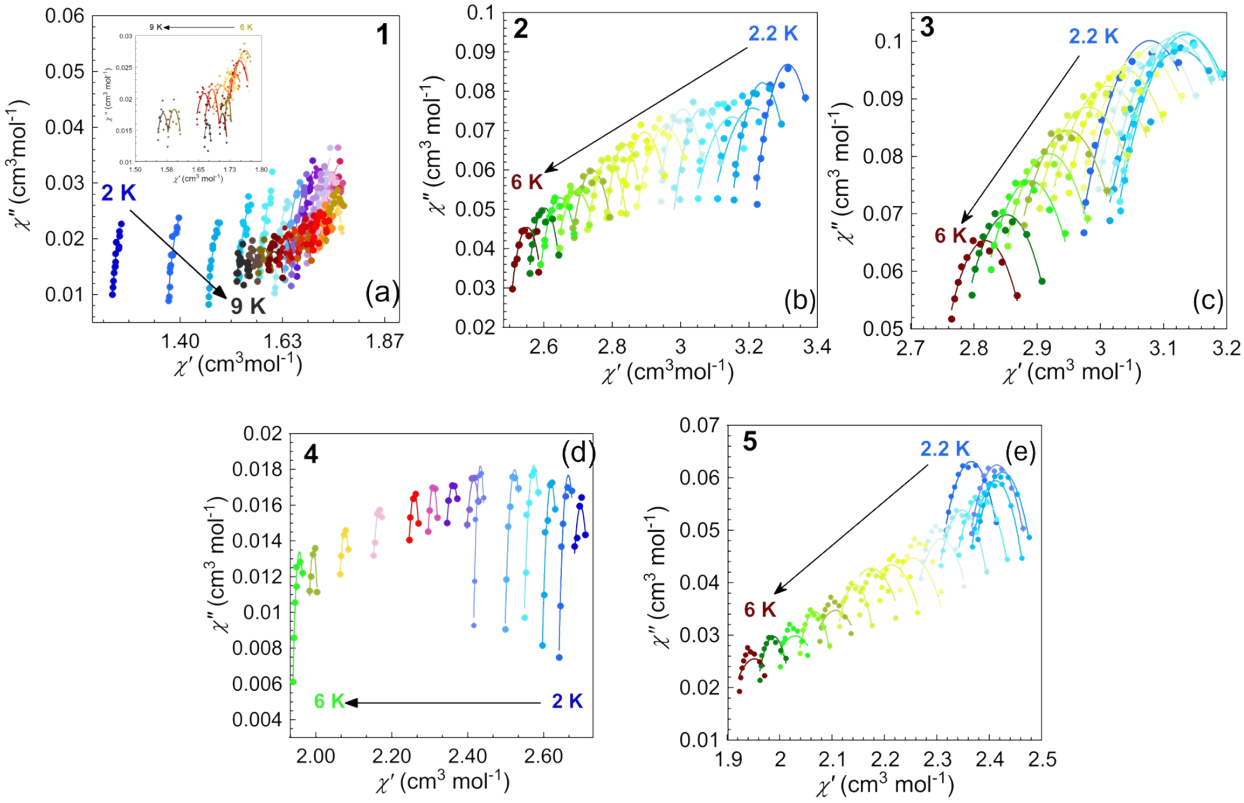

Fig. S26. Cole-Cole plots for **1**-**5** (a-e) at ±5 Oe oscillating field in the temperature range 2.0-9.0 K (**1**) (blue to dark grey) and 2.0-6.0 K (**2**-**5**) (blue to dark red) and under an applied static magnetic field of 1.0 (**1**) or 0.5 T (**2**–**5**). The inset shows the high-temperature data for **1** (a). The solid lines are the best-fit curves through the generalized Debye model (see text).

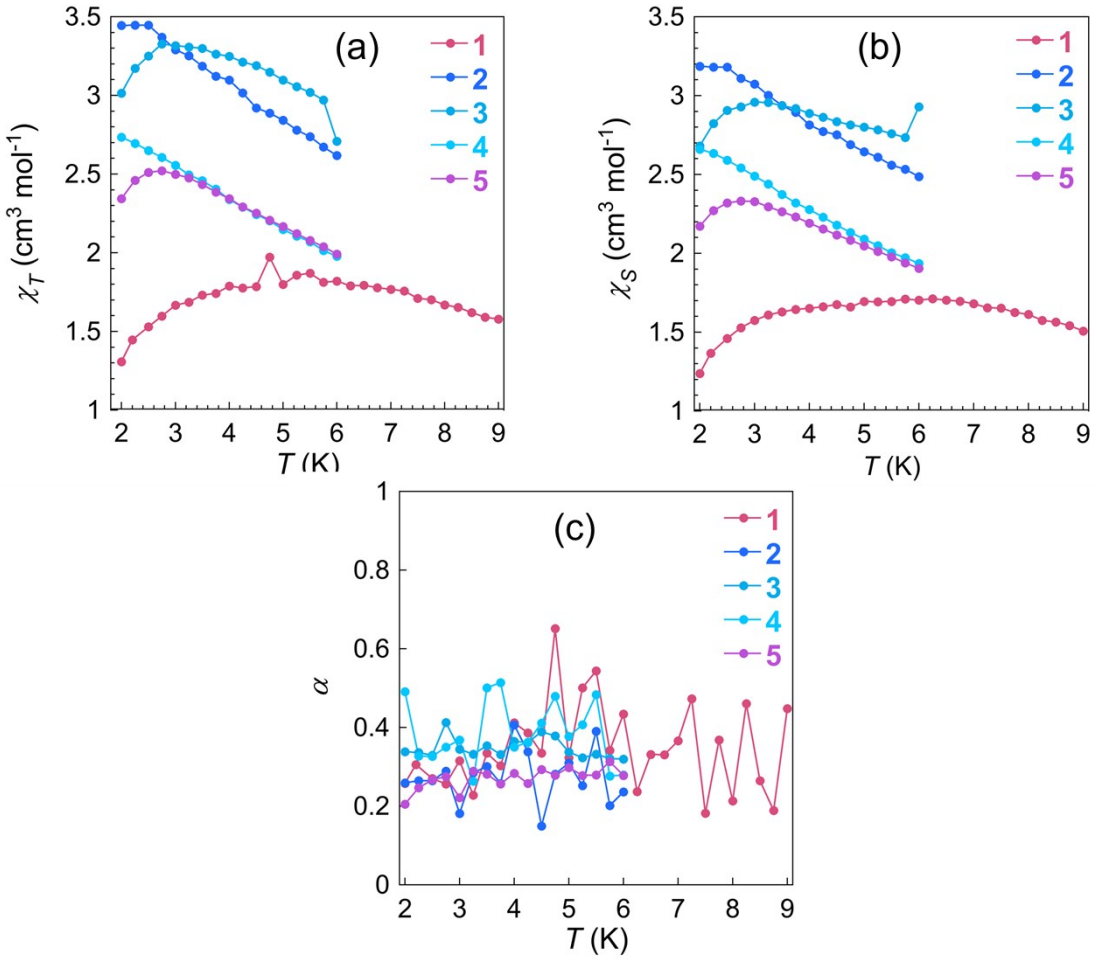

Fig. S27. Temperature dependence of χ_T (a), χ_S (b), and α (c) for **1-5** from the least-squares fitting of the Cole-Cole plots through the generalized Debye model (see text), under an applied static magnetic field of 1.0 T (**1**) and 0.5 T (**2-5**) in the temperature range 2-9 K (**1**) and 2-6 K (**2-5**).

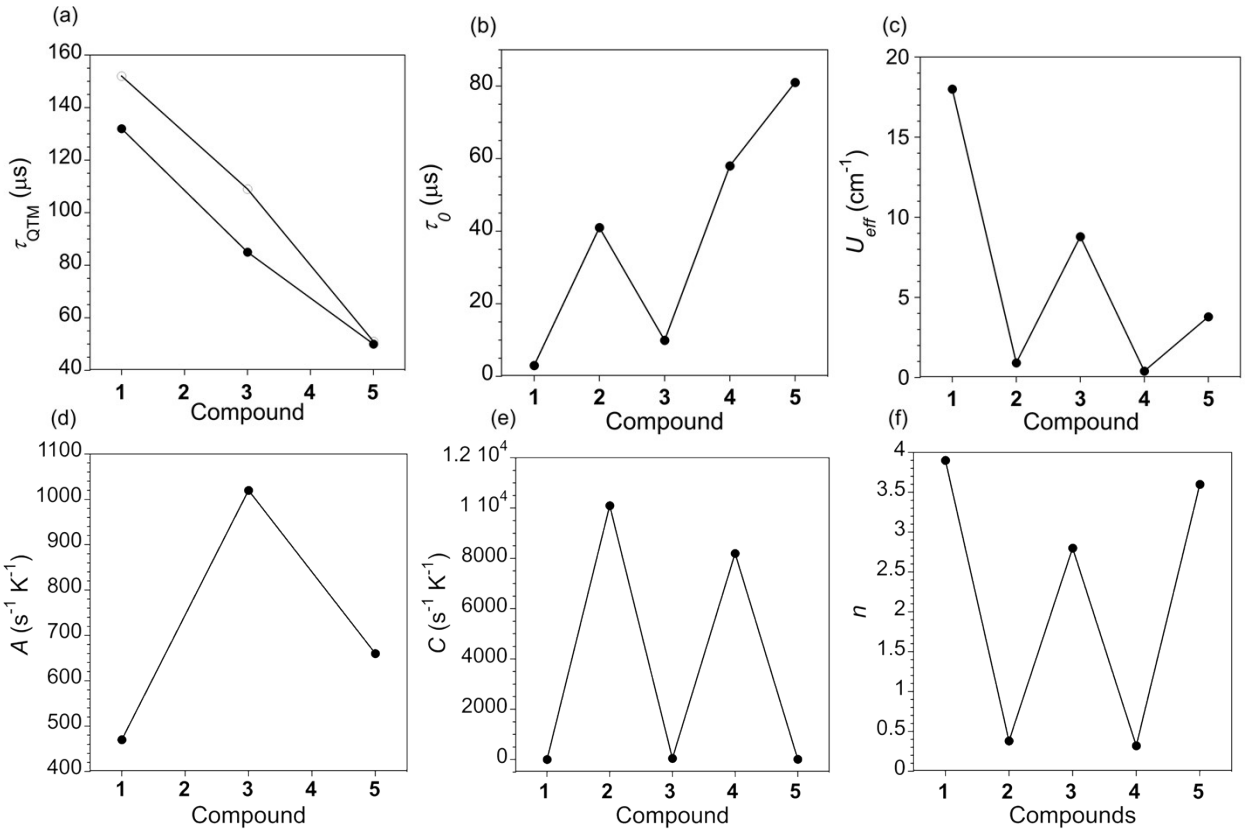

Fig. S28. Plots showing the variation of the values of τ_{QTM} (a), τ_0 (b), and U_{eff} (c), A (d), C (e), and n (f) for the QTM, and ORB, DIR, and RAM relaxation mechanisms of **1**-**5** (data from Table 3). The filled circles correspond to the fits through ORB (**2** and **4**) or ORB plus QTM (**1**, **3**, and **5**) mechanisms, while the open circles correspond to the fits through RAM (**2** and **4**) or RAM plus QTM and DIR (**1**, **3**, and **5**) mechanisms (b) (see text). The solid lines are only eye-guides.

Table S6. Selected magnetocaloric data for mixed-3d/nd 0D PBAs proposed as cryomagnetic refrigerants.

Compound[a]	M	M'	*x*	*y*	*N*[b]	*S*[c]	*D*[d] (K)	*T*[e] (K)	*H*[f] (T)	$-\Delta S_m$[g] (J kg^{-1} K^{-1})	Ref.
$\{Ni[Ni(dtbpy)(H_2O)]_8[W(CN)_8]_6\}\cdot 17H_2O$	Ni^{II} (HS)	W^{V}	9	6	15	12	0.07	5.3	7	3.8	91
$\{[Mn(tmphen)_2]_4[Nb(CN)_8]_2\}\cdot 14H_2O\cdot 7CH_3OH$	Mn^{II} (HS)	Nb^{IV}	4	2	6	9	0	2	7	8.3	92
$\{[Ni(H_2O)_2]_6[Ni(pyca)(H_2O)]_{12}[Fe(htpzb)(CN)_3]_{24}\}\cdot 2H_2O$	Ni^{II} (HS)	Fe^{III} (LS)	18	24	42	25	n.a.	8	7	8.3	93
$\{[Fe(H_2O)_2]_6[Fe(pyca)(H_2O)]_{12}[Fe(htpzb)(CN)_3]_{24}\}\cdot 6H_2O$	Fe^{II} (HS)	Fe^{III} (LS)	18	24	42	45	n.a.	7	7	16.2	93
$\{[Mn(H_2O)_2]_6[Mn(pyca)(H_2O)]_{12}[Fe(htpzb)(CN)_3]_{24}\}\cdot 4H_2O$	Mn^{II} (HS)	Fe^{III} (LS)	18	24	42	87/2	n.a.	3	7	17.7	93

[a]Ligand abbreviations: dtbpy = 4,4'-di-*tert*-butyl-2,2'-bipyridine, pyca = pyridyne-4-carboxylate, htpzb = hydrotris(pyrazolyl)borate, tmphen = 3,4,7,8-tetramethyl-1,10-phenanthroline. [b]Value of the nuclearity. [d]Value of the ground spin state calculated from the variable-field magnetization measurements. [d]Value of the axial magnetic anisotropy calculated from the variable-field magnetization measurements. [e]Value of the temperature. [f]Value of the magnetic field change. [g]Value of the maximum magnetic entropy change (in gravimetric units) estimated from indirect variable-field magnetization or heat capacity measurements.

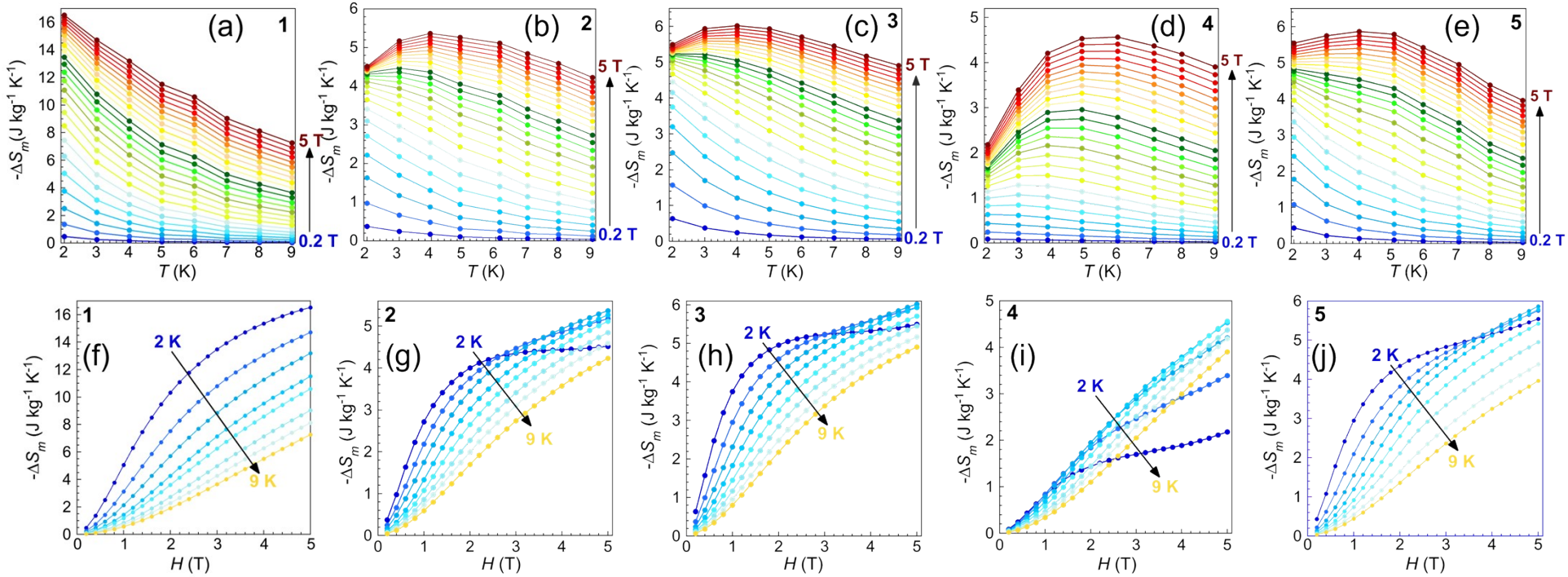

Fig. S29. Temperature (a-e) and field (f-j) dependence of $-\Delta S_m$ (in gravimetric units) for **1-5** in the field and temperature ranges of 0–5 T (blue to red) and 2.0-10 K (blue to orange), respectively,

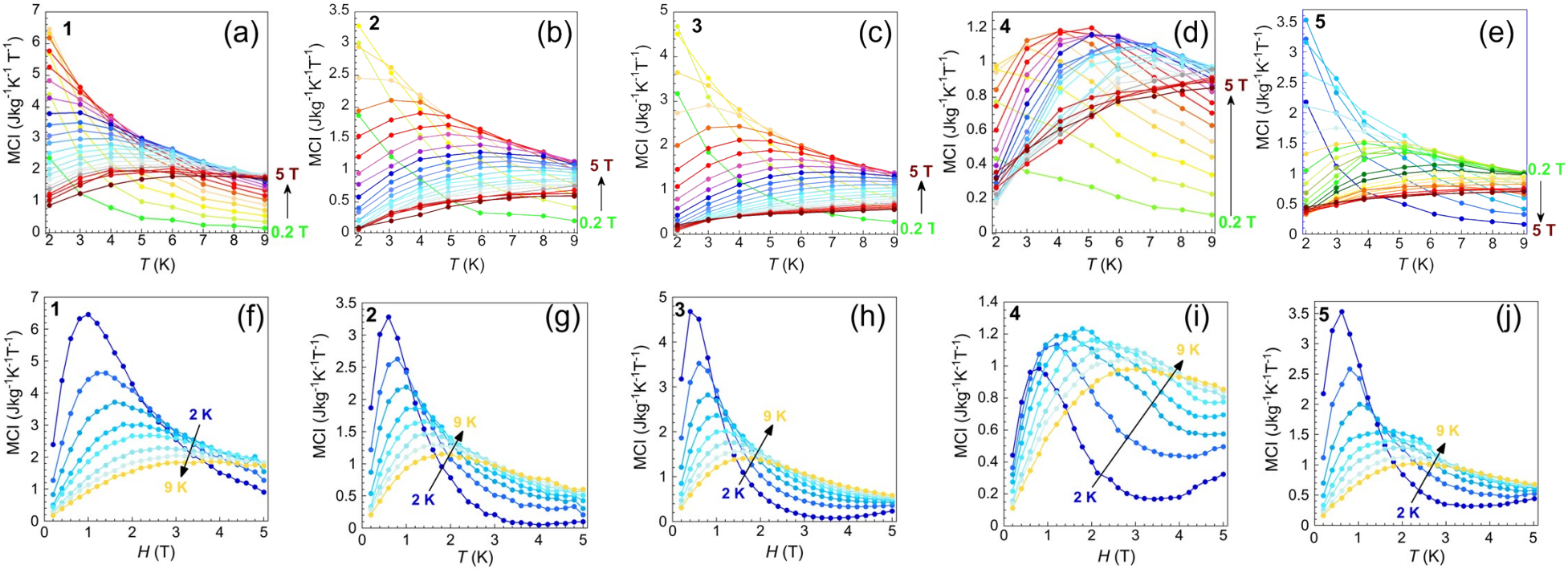

Fig. S30. Temperature (a-e) and field (f-j) dependence of the magnetocaloric efficiency index (MCI), defined as $-\partial(\Delta S_m)/\partial H$ (in gravimetric units), for 1-5 in the field and temperature ranges of 0–5 T (green to red) and 2-10 K (blue to yellow), respectively